

AD-A083 767

PURDUE UNIV LAFAYETTE IND PROJECT SQUID HEADQUARTERS  
FLOW FIELD MEASUREMENT USING RAMAN AND LDV TECHNIQUES.(U)  
APR 79 S LEDERMAN, A CELENTANO, J GLASER  
SQUID-PIB-36-PU

F/G 20/4

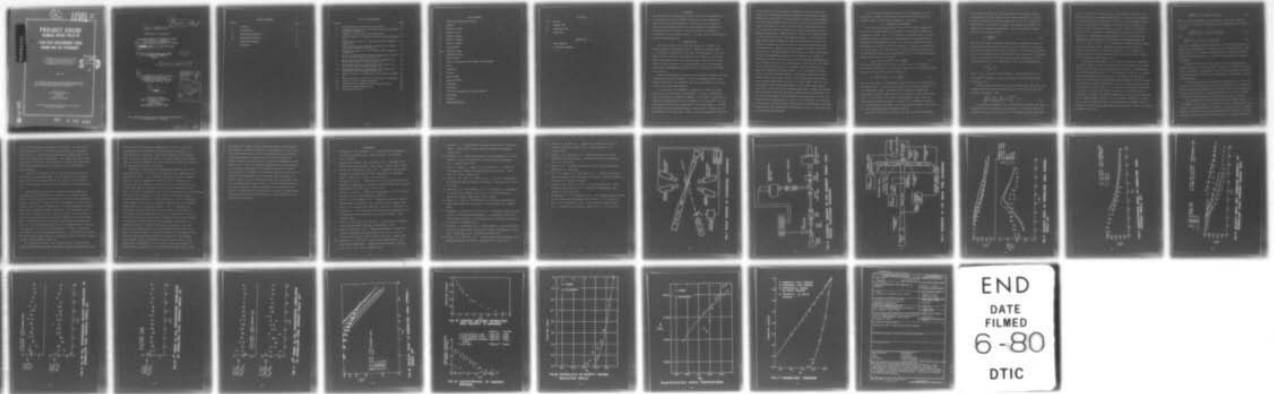
N00014-75-C-1143

NL

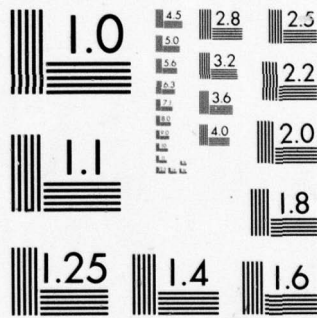
UNCLASSIFIED

| OF |

AD  
A083767



END  
DATE  
FILMED  
6-80  
DTIC



MICROCOPY RESOLUTION TEST CHART  
NATIONAL BUREAU OF STANDARDS-1963-A

12

LEVEL II

ADA 083767

# PROJECT SQUID

## TECHNICAL REPORT PIB-36-PU

### FLOW FIELD MEASUREMENT USING RAMAN AND LDV TECHNIQUES

S. LEDERMAN, A. CELENTANO, J. GLASER  
AERODYNAMICS LABORATORIES  
POLYTECHNIC INSTITUTE OF NEW YORK  
FARMINGDALE, NEW YORK 11735

SDTIC  
ELECTE  
APR 29 1980  
S D  
E

APRIL 1979

Project SQUID is a cooperative program of basic research relating to Jet Propulsion. It is sponsored by the Office of Naval Research and is assisted by Purdue University through Contract N00014-75-C-1143, NR-098-038.

Published for ONR by  
School of Mechanical Engineering  
Chaffee Hall  
Purdue University  
West Lafayette, Indiana 47907

This document has been approved for public release and sale;  
its distribution is unlimited.

DDC FILE COPY

80 4 29 042

9 Interim report

4 Technical Report, PIB-36-PU

PROJECT SQUID

A COOPERATIVE PROGRAM OF FUNDAMENTAL RESEARCH  
AS RELATED TO JET PROPULSION  
OFFICE OF NAVAL RESEARCH, DEPARTMENT OF THE NAVY

15 ~~CONTRACT~~ N00014-75-C-1143 NR-098-038

6 FLOW FIELD MEASUREMENT USING RAMAN  
AND LDV TECHNIQUES

12 37

By 14 SQUID-PIB-36-PU

10 S. Lederman, A. Celentano, J. Glaser  
Aerodynamics Laboratories  
Polytechnic Institute of New York  
Farmingdale, New York 11735

11 April 1979

Accession For	
NTIS GRA&I	<input checked="" type="checkbox"/>
DDC TAB	<input type="checkbox"/>
Unannounced	<input type="checkbox"/>
Justification	
By _____	
Distribution/	
Specialty Codes	
Dist	Avail and/or special
A	

Published for ONR by  
School of Mechanical Engineering  
Chaffee Hall  
Purdue University  
West Lafayette, Indiana 47907

This document has been approved for public release and sale;  
its distribution is unlimited.

403677 slt

## TABLE OF CONTENTS

Section		Page
	Abstract	1
I	Introduction	1
II	Theoretical Background	3
III	Experimental Apparatus	8
IV	Experimental Results	8
	References	12

LIST OF ILLUSTRATIONS

Figure		Page
1	Block Diagram of Experimental Apparatus	15
2	Schematic Diagram of the Coherent Raman Anti-Stokes Scattering Apparatus	16
3	Schematic of the Shock Tube Experiment	17
4	Velocity Ratio vs. Normalized Axial Distance-Single Jet	18
5	Concentration Ratio vs. Normalized Axial Distance-Single Jet	19
6	Velocity Ratio and Turbulent Intensity vs. Normalized Axial Distance-Coaxial Jet	20
7	Concentration Ratio vs. Normalized Axial Distance-Coaxial Jet	21
8	$N_2$ or $CO_2$ Concentration-Velocity Magnitude Correlation vs. Axial Distance-Single Jet	22
9	$N_2$ or $CO_2$ Concentration-Velocity Correlation vs. Normalized Axial Distance-Single Jet	23
10	First Order $N_2$ - $CO_2$ Concentration Correlation vs. Normalized Axial Distance-Single Jet	24
11	Second Order $N_2$ - $CO_2$ Concentration Correlation vs. Normalized Axial Distance-Single Jet	25
12	Velocity Ratio vs. Normalized Axial Distance-Single Jet	26
13	Unburnt Methane Normalized with Respect to Maximum	27
14	Concentration of Unburnt Methane	27
15	Normalized $N_2^+$ Density Behind Reflected Shock	28
16	Reflected Shock Temperatures	29
17	Normalized Pressure	30

## LIST OF SYMBOLS

A	Interaction cross-sectional area
C	Constant
c	Velocity of light
d	Diameter of jet
$f_d$	Doppler frequency
$f_i$	Number of samples i
h	Plancks' constant
I	Line intensity
$l_{coh}$	Coherence length
k	Boltzmann constant
N	Number density
n	Index of refraction or total number of observations
$\rho$	Power
T	Temperature
u, V	Velocity
X	Axial position
$\Gamma_r$	Raman line width
$\lambda$	Wavelength
$\nu$	Wave number
$\sigma$	Scattering cross-section, tubulent intensity
$\Omega$	Solid angle
$\omega$	Frequency
$\chi$	Raman susceptibility

### Subscripts

$\alpha, \beta$  Species  
o Incident line  
AS Anti-Stokes line  
s Stokes line

### Superscripts

- Mean component  
' Fluctuating component

## ABSTRACT

The application of spontaneous Raman, CARS and LDV techniques to a wide spectrum of flow fields confirms the basis hypothesis, that these laser based diagnostic techniques have a very wide range of applicability and can be instrumental in providing experimental data in friendly as well as hostile environments unobtainable by conventional means. The data can be obtained non-intrusively and remotely.

### I. INTRODUCTION

As is well known, the final performance of a system, can seldom exceed the performance of its component building blocks. It is therefore essential for the sake of performance of the complete system to optimize the design and performance of the individual building blocks of the given system. While this is a generally accepted practice, it is particularly true in the design and ultimate performance characteristics of propulsion and combustion systems.

While many computer codes have been developed dealing with combustion and propulsion devices, it must be remembered that most theoretical models are idealized and their reliability can only be verified by proper measurements.

In some cases the parameters necessary to evaluate a given model must be determined experimentally. If this is impossible these parameters are generally assumed. Furthermore, comparison of computed and measured over-all performance of a given device is an insensitive test for the correctness of the model (Ref. 1) and does not permit the self-identification of the specific reasons for the discrepancies that may exist. Many factors may adversely affect the

performance of devices based on combustion and flow properties. Among these the boundary layers, turbulence, insufficient mixing, inadequate combustion, fluctuation due to combustor instabilities etc. may cause undesired and sometimes unexpected results, which may be detrimental in terms of the over-all system performance. It is therefore not only desirable but almost imperative to have adequate measurement capabilities not only at each building block of the system but also on the complete system. To be effective these measurement capabilities must have sufficient spacial and temporal resolution, must be specific, and most importantly must be nonintrusive. These can only be achieved by means of optical diagnostics. The development of the latter, for flow fields under adverse environmental conditions as encountered in a number of propulsion devices, has been the aim of continuing investigations for a number of years in the Aerodynamics Laboratories of the Polytechnic Institute of New York, and many other laboratories, and have been supported by Project SQUID. As a consequence of these efforts the laser based diagnostic techniques consisting of spontaneous Raman scattering, coherent anti-Stokes Raman scattering, laser Doppler velocimetry etc. have been developed. Some of these techniques provide the experimentalist with capabilities, which were only a short time ago considered impossible. Among the measurements possible using the previously mentioned laser techniques, are the remote simultaneous and instantaneous measurement of specie concentration and temperature at a point in the flowfield, the velocity at that point, and the derived variables such as turbulence intensity, concentration and temperature fluctuation, as well as correlation and crosscorrelation parameters.

In this report a summary of some of the developments in our laboratory in terms of the measurables and some typical data obtainable using the available equipment is presented.

## II. THEORETICAL BACKGROUND

The theoretical background of the Raman scattering techniques as well as the laser Doppler velocimeter techniques is presented adequately in Refs. 8-15. It is therefore sufficient here to recall the basic governing equations concerning specie concentration and temperature measurements by means of the Raman effect and velocity measurements by means of the LDV techniques. Thus, the concentration of a given specie in a mixture may be obtained from the intensity of the vibrational Stokes or or anti-Stokes line of the scattered laser energy by the specie of interest:

$$I_{S,A} = CN I_0 (\nu_0 \pm \nu)^4 [1 - \exp(-\frac{h\nu}{kT})]^{-1} \quad (1)$$

To obtain the temperature one may use the ratio of the Stokes to anti-Stokes intensity for a given specie, which at equilibrium taking account of the Boltzman factor results in:

$$T = \frac{h\nu c}{k} \left[ \ln \frac{I_S}{I_A} + 4 \ln \left( \frac{\nu_0 + \nu}{\nu_0 - \nu} \right) \right]^{-1} \quad (2)$$

One may also obtain the temperature from the ratios of intensities of rotational lines, or from the hot bands of the resolved Q-branch of the vibrational lines. These and other methods of temperature measurement using the Raman effect are discussed in the cited references. In any case, it is clear from equations 1 and 2 that the concentration and temperature of a specie in a flowfield is measurable nonintrusively, and when a high power short duration laser pulse is used, instantaneously and simultaneously.

As far as the LDV is concerned, Ref. 15 it is well known that

the theoretical basis for this technique is the Doppler effect. Assuming that all the conditions for proper operation of the LDV are met, including the proper number and size of the scattering particles in the scattering volume, the velocity measurement is reduced to a frequency measurement. For a dual scatter Doppler system the frequency becomes:

$$f_d = \frac{2V \sin \theta / 2}{\lambda_o} \quad (3)$$

The velocity signals obtained from frequency signals processed appropriately can be stored in the form of a histogram in the memory of an on-line computer and later processed to yield desired information. Thus with the usual definition of the velocity in a turbulent flow as consisting of the mean and fluctuating component  $u = \bar{u} + u'$ , the mean velocity in a 1 dimensional L.D.V. may be obtained from

$$\bar{u} = \frac{1}{n} \sum_{i=1}^k f_i u_i \quad (4)$$

where  $n = \sum_{i=1}^k f_i$  is the total number of observations, and  $f_i$  is the number of samples of the total number of observations having the velocity  $u_i$ .

From the mean velocity and the stored individual velocities the standard deviation may be obtained which is nothing less than the turbulent intensity. Thus

$$\sigma = \left[ \frac{n \sum_{i=1}^k f_i u_i^2 - \left( \sum_{i=1}^k f_i u_i \right)^2}{n(n-1)} \right]^{1/2} = \overline{u'^2} \quad (5)$$

As indicated previously, the concentration of species and their temperature can be obtained instantaneously (~10-15nsec) and simultaneously using the high power short time duration laser pulse tech-

nique by means of the Raman effect. The question arises if it is possible from the instantaneous Raman data to deduce some information concerning the concentration (density) and temperature fluctuation in a flow field? To answer that question one need only consider the data reduction scheme of the LDV. The mean velocity is obtained from a histogram of individual velocities according to equation 4. Proceeding the same way with the concentration and temperature data which may be defined in an analogous manner as  $C = \bar{C} + C'$  and  $T = \bar{T} + T'$ , it is possible to obtain the mean concentration and temperature. Continuing the same way as with the velocity fluctuation or turbulent intensity, it is possible to utilize equation 5 again and obtain the concentration and temperature fluctuation in the given flow.

It has been shown (Hilst, et al, Gupta and Wakelyn, Donaldson and Varma) that in chemically reacting flows "the effects of concentration fluctuations can be significant to the point of dominating the chemical reaction rates". It is pointed out that for a strongly skewed distribution of  $C_\alpha$  and  $C_\beta$  in a two specie reaction case, where the concentration fluctuations become dominant the third order correlations of these distributions must be included in the generalized chemical kinetic model. In the case of a turbulent chemically reacting flow, where the reaction rates are fast and the scale of turbulence is large, the reaction model based on mean value chemistry may be substantially in error. It is therefore necessary in chemically active turbulent flows to include second and higher order correlations involving the concentration fluctuations. These, as defined by Hilst et al, are:

$$\overline{C_{\alpha} C_{\beta}} = \frac{1}{N} \sum_i n_i (C_{\alpha i} - \bar{C}_{\alpha}) (C_{\beta i} - \bar{C}_{\beta}) \quad (6)$$

where  $n_i$  is the frequency of occurrence of the joint values of  $C_{\alpha i}$ ,  $C_{\beta i}$ ,  $N = \sum_i n_i$  and  $C_{\alpha}$  and  $C_{\beta}$  are the concentrations of species  $\alpha$  and  $\beta$ .

$$\overline{C_{\alpha}^2 C_{\beta}} = \frac{1}{N} \sum_i n_i (C_{\alpha i} - \bar{C}_{\alpha})^2 (C_{\beta i} - \bar{C}_{\beta}) \quad (7)$$

and

$$\overline{C_{\alpha} C_{\beta}^2} = \frac{1}{N} \sum_i n_i (C_{\alpha i} - \bar{C}_{\alpha}) (C_{\beta i} - \bar{C}_{\beta})^2 \quad (8)$$

Since the spontaneous Raman effect used as indicated previously is capable of providing the concentrations and temperatures of a number of species in a mixture simultaneously, a simple processing procedure according to eq. 6, 7 and 8 would provide the desired parameters.

With all of the basic data stored in the data acquisition memory system, it is quite simple to construct a number of correlations of interest, for example, a correlation between the velocity and concentration, velocity and temperature or temperature and concentration etc.

In situations where the spontaneous Raman signal is low, be it due to low concentration of the specie of interest or low primary power available or allowable to be applied, and the subsequent low signal to noise ratio, a nonlinear Raman process, the so called Coherent anti-Stokes Raman scattering process may be utilized.

The coherent anti-Stokes Raman scattering (CARS) (Begley, et al, Reguier, et al, Moya, et al) process may be quantitatively described as a process by which a photon  $\nu_1$  interacts with a tunable photon  $\nu_2$  (Stokes photon of the given specie of interest) through the third order non-linear susceptibility to generate a polariza-

tion component of the anti-Stokes frequency  $\nu_3 = 2\nu_1 - \nu_2$ .

Quantitatively the anti-Stokes scattered power can be shown to be represented by:

$$P_{AS} = \frac{2.77 \cdot 10^{-3}}{n_{AS}^4 \lambda_{AS}^2} \left( \frac{\ell_{coh}}{A} \right)^2 [N\chi]^2 P_L^2 P_S \quad (9)$$

The coherence length  $\ell_{coh}$  defined as  $\pi/\Delta k$  where  $\Delta k = 2k_1 - k_2 - k_3$  may be written as

$$\ell_{coh} = \frac{\pi c}{v_{vibr}^2} \left[ 2 \frac{\partial n}{\partial \nu} + \nu_L \frac{\partial^2 n}{\partial \nu^2} \right] \quad (10)$$

and the Raman susceptibility  $\chi$  may be expressed as

$$\chi = \frac{2\pi^2 C^4}{h\omega_L \omega_s^3 \Gamma_R} \frac{d\sigma}{d\Omega} \quad (11)$$

It is clear from equation 9 that unlike the relation of Eq. 1, the scattered radiation is not only nonlinearly related to the specie concentration but also nonlinearly related to the incident radiation. Furthermore, those are not the only negative features of the CARS process in comparison with the spontaneous Raman process. To mention only two, the CARS process is not single ended like that of the spontaneous Raman, where the transmitter and receiver may use the same optics or may be located in proximity to each other. The spontaneous Raman techniques permits the measurement of many species which may be present in a given system simultaneously using a single primary laser. This is not possible with the CARS diagnostic method. These negative features of CARS are offset by the much higher equivalent scattering cross section. In some cases as much as nine orders of magnitude higher than the spontaneous Raman effect. This feature alone makes in some instances the difference between

performing a difficult measurement or not performing it at all. In a later section an example of such a measurement will be shown.

### III. EXPERIMENTAL APPARATUS

The experimental apparatus utilized in this work is shown diagrammatically in Fig. 1, 2 and in Fig. 3. A complete description of the apparatus of Fig. 1 and 2 is given in Refs. 1,11. The individual components are indicated on the schematic diagrams.

The apparatus of Fig. 3 present a schematic diagram of an experiment where the temperature and concentration of an ionized specie behind a reflected shock in a shock tube are measured. As is clear from the figure, a Ruby laser pulse is incident at the reflected shock in the shock tube, and the Stokes and anti-Stokes radiation of an ionized specie is measured at  $90^\circ$  to the incident radiation. Here a 1 joule Ruby laser as shown in Fig. 2 is utilized in combination with proper synchronization and measuring photo-multiplier tubes. The data are fed to the data acquisition system, where it is processed, reduced and presented in the appropriate form.

### IV. EXPERIMENTAL RESULTS

With the apparatus described, a series of tests have been conducted. The purpose of these tests was the demonstration of the applicability of the integrated Raman-LDV system and the presentation of some turbulence related data obtainable from the pulsed Raman system, as well as the ability to obtain some correlation data. Thus Fig. 4 presents normalized axial velocity profiles and turbulence intensities of a single jet. Fig. 5 shows the normalized concentration profiles of a single jet. Fig. 6 presents normalized velocity profiles in a coaxial turbulent diffusion jet and flame followed in Fig. 7 by the normalized axial concentration profiles of  $N_2$  of the

same coaxial turbulent diffusion jet and flame. In Figures 8-11 data correlations of the first and second order are presented. These relate to concentration-concentration correlations and to velocity concentration correlations. The significant point about those data is that they were obtained in reactive and nonreactive flow fields nonintrusively and therefore may be considered as quite reliable.

In Fig. 12 a normalized plot of the velocity profiles in a cold jet and a flame are shown. The intersection of the axis of the jet by the data line indicates the length of the potential core, and the slope of the line the exponential law describing the jet.

As mentioned previously, the spontaneous Raman diagnostic technique has some limitations in terms of the signal to noise ratio. In cases where the concentration is low or the permissible applied laser power is limited or the environment is such that the signal to noise ratio is insufficient to perform meaningful measurements using spontaneous Raman diagnostics, the CARS system may be very useful. Figures 13 and 14 show the results of measurements in sooty air methane flames of the unburnt methane in the flame using CARS. No response could be obtained using spontaneous Raman diagnostics. It is worthwhile noting that the maximum methane concentration measured at  $X/d = 1$  was insufficient to produce a measurable reproducible signal using spontaneous Raman. The CARS system utilized here was of the coaxial type as is apparent from the schematic diagram of Fig. 2 and discussed in Ref. 11.

To indicate the scope of the applicability of the high power single pulse spontaneous Raman diagnostic technique an experiment has

been conducted as indicated schematically in Fig. 3. Here the temperature and concentration of ionized species behind a reflected shock are measured. While other methods for the measurement of the gas properties behind a reflected shock are available, Refs. 16-18 this experiment has been conducted to show the scope of the applicability of this technique.

Thus Fig. 15 indicates the normalized  $N_2^+$  density behind the reflected shock as a function of incident Mach no. compared to the theoretical values. As is evident, with the increase in incident Mach. no. and the consequent increase of the no. density, the measured and the computed concentration fall closer together, and at the upper end of the measured interval the agreement is quite good. The same is apparently true for the temperature Fig. 16 behind the reflected shock although to a lesser extent in absolute limits. The higher number density of the ionized specie and the consequent higher signal to noise ratio evidently contribute to more reliable measurements at the upper Mach number. Fig. 17 indicates the normalized total pressure and partial pressure of  $N_2^+$  compared to the computed values predicted by theory. At this point it must be noted that while the concentration of  $N_2^+$  behind the reflected shock at higher Mach numbers exhibits good agreement with theory, the temperature which is obtained according to Equation 2, from the ratio of the Raman Stokes to the anti-Stokes intensity still exhibits excessive scatter. Here it is believed the bandpass of the available anti-Stokes filter which was higher than the bandpass of the Stokes filter contributed to some excessive noise. This measurement, irrespective of the absolute values, establishes in principle the applicability of the spontaneous Raman effect to the

measurement of ionized species and temperatures nonintrusively and remotely. The shock tube data, considering the size of the shock tube used, the size of the access windows and the difficulties encountered in general in any limited accessibility system, indicate that those remote nonintrusive diagnostic techniques, are at this time working techniques that can be applied to a variety of problems and invaluable data may be obtained utilizing these techniques. This however, does not mean that all problems associated with those techniques have been fully resolved. There is still a great deal that can and should be done. It is possible that a major portion of the outstanding problems associated with those remote techniques can be solved in the process of applying those techniques to practical problems, which require experimental data and which were unobtainable with the conventional techniques.

#### REFERENCES

1. Bornstein, J. and Lederman, S.: "Experimental Investigation of Coaxial Turbulent Jets: Israel Journal of Technology, Vol. 14, 1976.
2. Begley, R.F., Harvey, A.B. and Beyer, R.L.: "Coherent Anti-Stokes Raman Spectroscopy". Appl. Phys. Letters, 20, 7, 1974.
3. Coleman duP. Donaldson, Varma, A.K.: "Remarks on the Concentration of a Second Order Closure Description of Turbulent Flows". Comb. Sci. & Tech., Vol. 13, 1976.
4. Eckbreth, Allen C.: "Applicability of Laser Raman Scattering Diagnostics Techniques to Practical Combustion Systems", Project SQUID Report No. UTRC-4-PU, October 1976.
5. Goulard, R. Editor: "Combustion Measurements in Jet Propulsion Systems", Project SQUID Workshop, May 1975.
6. Gupta, R.N. and Wakelyn, N.T.: "Theoretical Study of Reactive and Nonreactive Turbulent Jets", NASA TN D-8127, August 1976.
7. Hilst, G.R., Coleman duP. Donaldson, Teske, M., Contiliano, R., Freiberg, J.: "The Development and Preliminary Applications of an Invariant Coupled Diffusion and Chemistry Model", NASA CR-2297, 1973.
8. Lapp, M., and Penny, C.M., Editors: "Laser Raman Gas Diagnostics", Project SQUID Workshop, Plenum Press, 1973.
9. Lapp, M. and Penny, C.M.: "Raman Measurements on Flames Advances in Infrared and Raman Spectroscopy, Vol. 3, ed. by R.J.H. Clark and R.E. Hester, Hyden & Son Ltd., London, 1977.
10. Lederman, S.: "The Use of Laser Raman Diagnostics in Flow Fields and Combustion". Progress Energy Combustion Science, Vol. 3, pp. 1-34, 1977, Pergamon Press.

11. Lederman, S.: "Experimental Techniques Applicable to Turbulent Flows". AIAA 15th Aerospace Sciences Meeting, Los Angeles, January 1977.
12. Lederman, S.: "Some Applications of Laser Diagnostics to Fluid Dynamics", AIAA 14th Aerospace Sciences Meeting, Washington, D.C., January 26-28, 1976.
13. Moya, F., Druet, S., Pealat, M., and Taran, Y.P.: "Flame Investigation by Coherent Antistokes Raman Scattering". AIAA Paper No. 76-29, January 1976.
14. Reguier, P.R., Moya, F., Taran, Y.P.E.: "Gas Conc. Measurement by Coherent Raman Antistokes Scattering". AIAA Paper No. 73-702, July 1973.
15. Stevenson, W.H. and Thompson, H.D.: Proceedings of a Workshop in the Use of Laser Doppler Velocimeter for Flow Measurements, March 1972, Purdue University, Project SQUID.
16. Glass, I.I., Editor: Proceedings of the Seventh International Shock Tube Symposium, University of Toronto Press, pp. 662-818, 1969.
17. Lederman, S., Abele, M. and Visich, M.: "Microwave Techniques Applicable to Shock Tube Measurements". Proceedings of the First International Congress on Instrumentation in Aerospace Simulation Facilities. September 1964.
18. Lederman, S. and Dawson, E.F.: "Application of a Microwave Technique to the Measurement of Electron Density and Relaxation Time". Phys. Fluids 10, 12, pp. 2570-2578, December 1967.
19. Barnett, D.O. and Giel, T.V.: "Laser Velocimeter Measurements in Moderately Heated Jet Flows", AEDC-TR-76-156, April 1977.

20. Chen, C.J. and Redi, W.: "A Review of Experimental Data of Vertical Turbulent Buoyant Jets". ITHM Report No. 193, October 1976.
21. Chigier, N.A. and Frokin, V.: "Mixing Processes in a Free Turbulent Diffusion Flame". Combustion Science and Tehnology Vol. 9, p. 111, 1974.
22. Harsha, P.T.: "A General Analysis of Free Turbulent Mixing". AEDC-TR-73-177, May 1974.
23. Lau, J.C., Morris, P.J. and Fisher, M.J.: "Turbulence Measurements in Subsonic and Supersonic Jets Using a Laser Velocimeter". AIAA Paper No. 76-348, July 1976.
24. Launder, B.E., Morse, A., Rodi, W. and Spalding, D.B.: "Free Turbulent Shear Flows, Vol. I, Conference Proceedings, NASA SP-321, p. 361, July 1972.
25. Morgenthaler, J.H. and Zelanay, S.W.: "Free Turbulent Shear Flow". Vol. 1 Conference Proceedings, NASA SP-321, p. 277, July 1972.
26. Rudy, D.H. and Bushnell, D.M.: "Free Turbulent Shear Flows". Vol. I, Conference Proceedings, NASA SP-321, p. 67, July 1972.

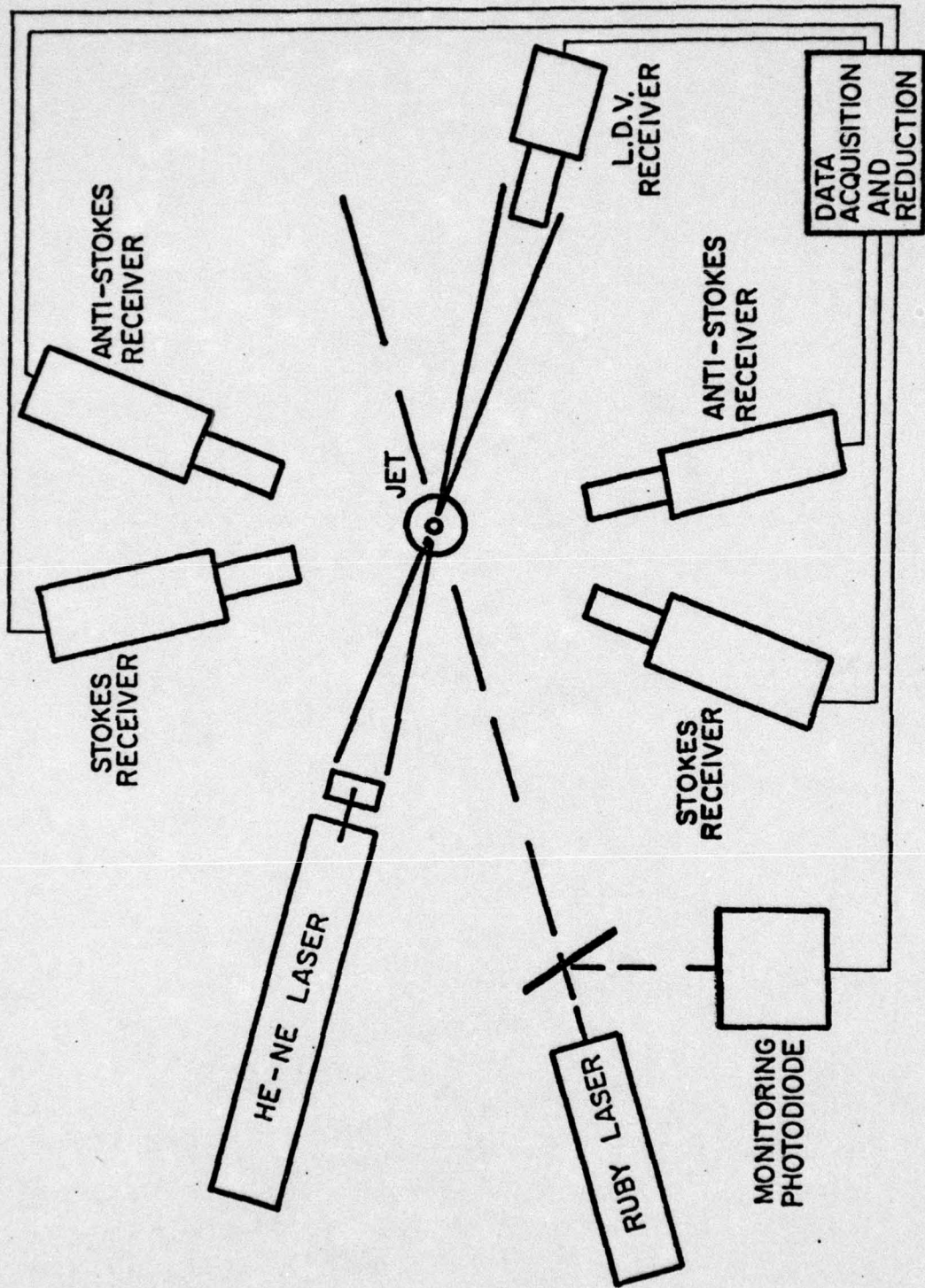


FIG. 1 BLOCK DIAGRAM OF EXPERIMENTAL APPARATUS

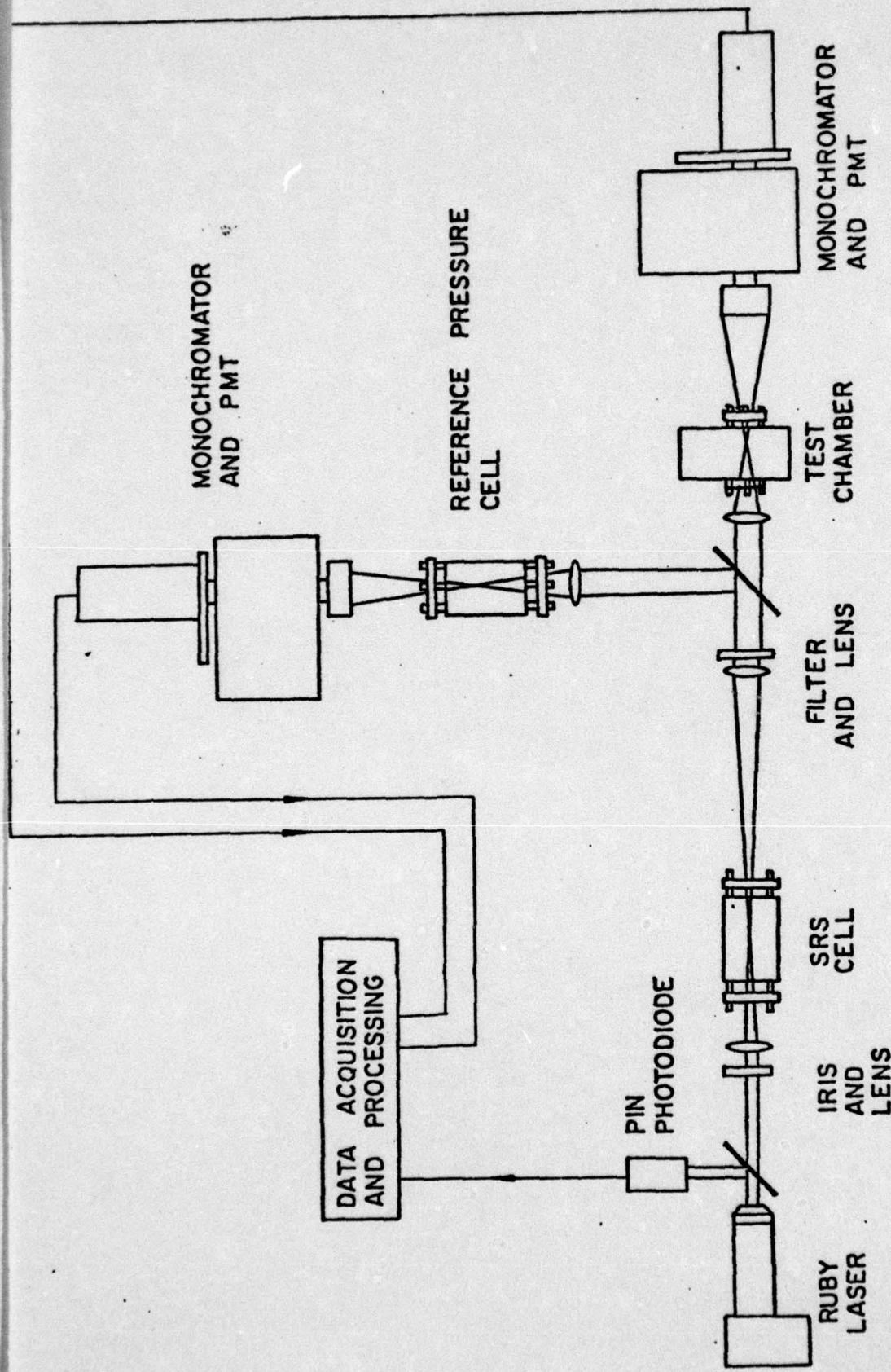


FIG. 2 SCHEMATIC DIAGRAM OF THE COHERENT RAMAN ANTI-STOKES SCATTERING APPARATUS

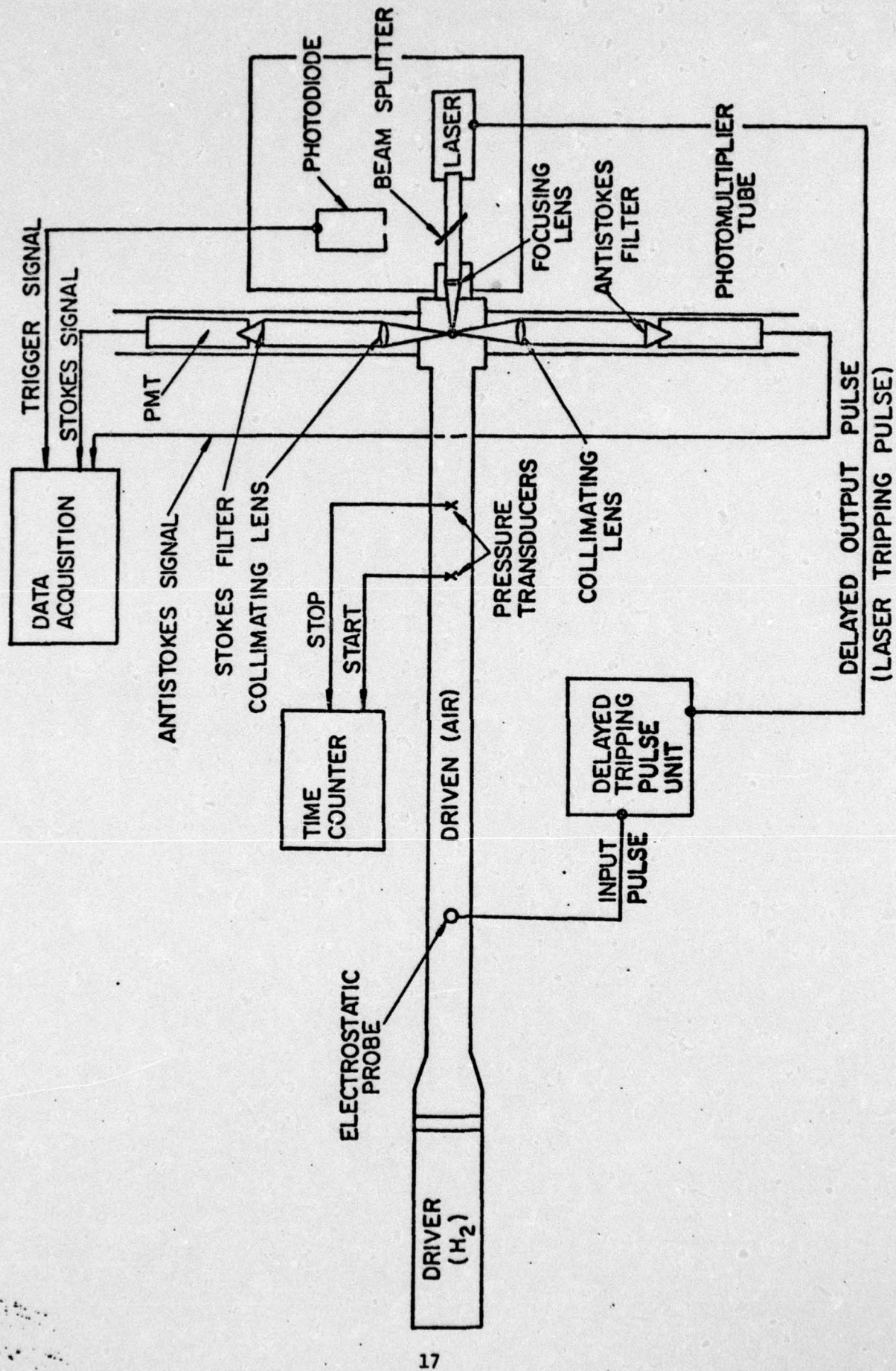


FIG. 3 SCHEMATIC OF THE SHOCK TUBE EXPERIMENT

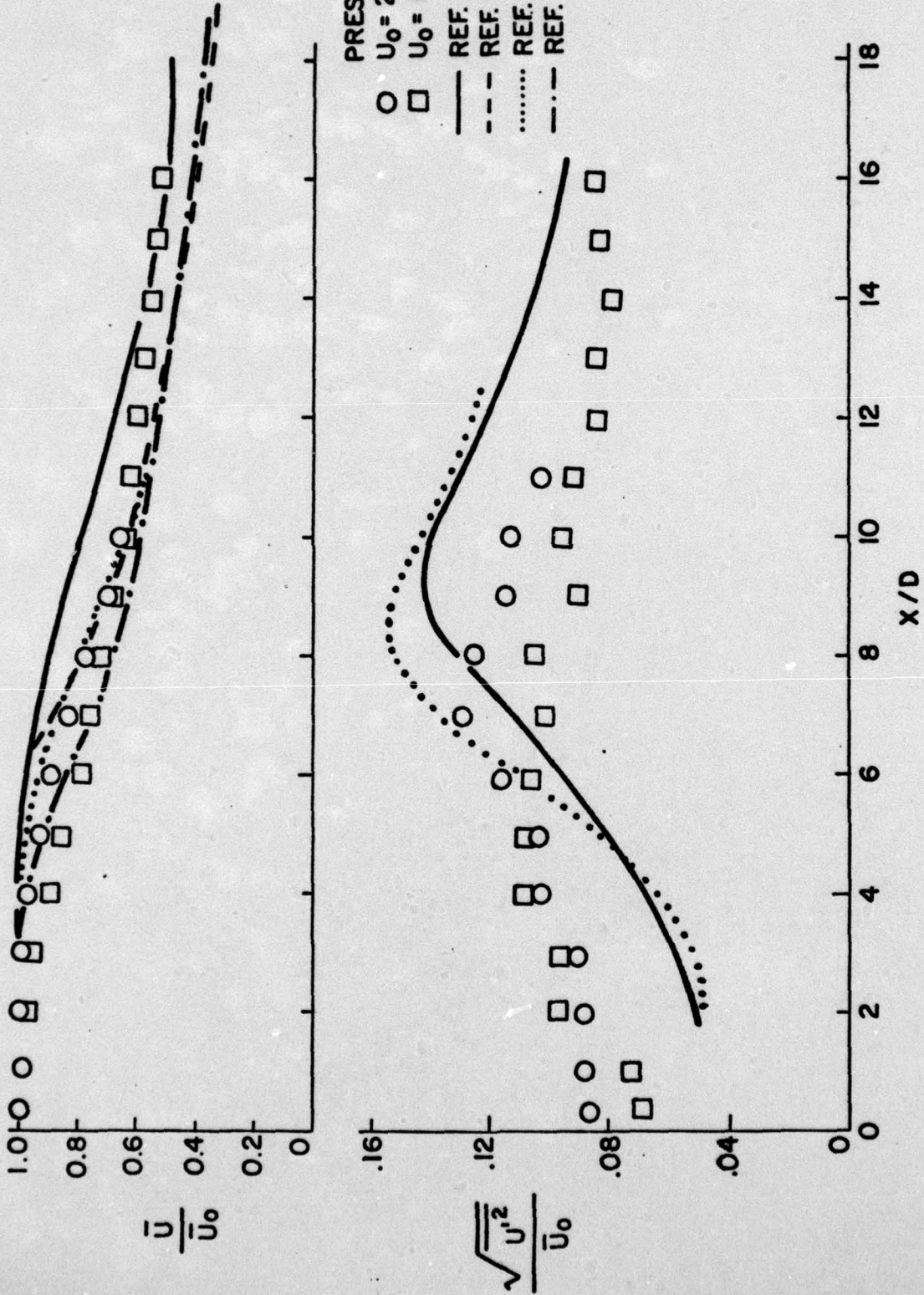
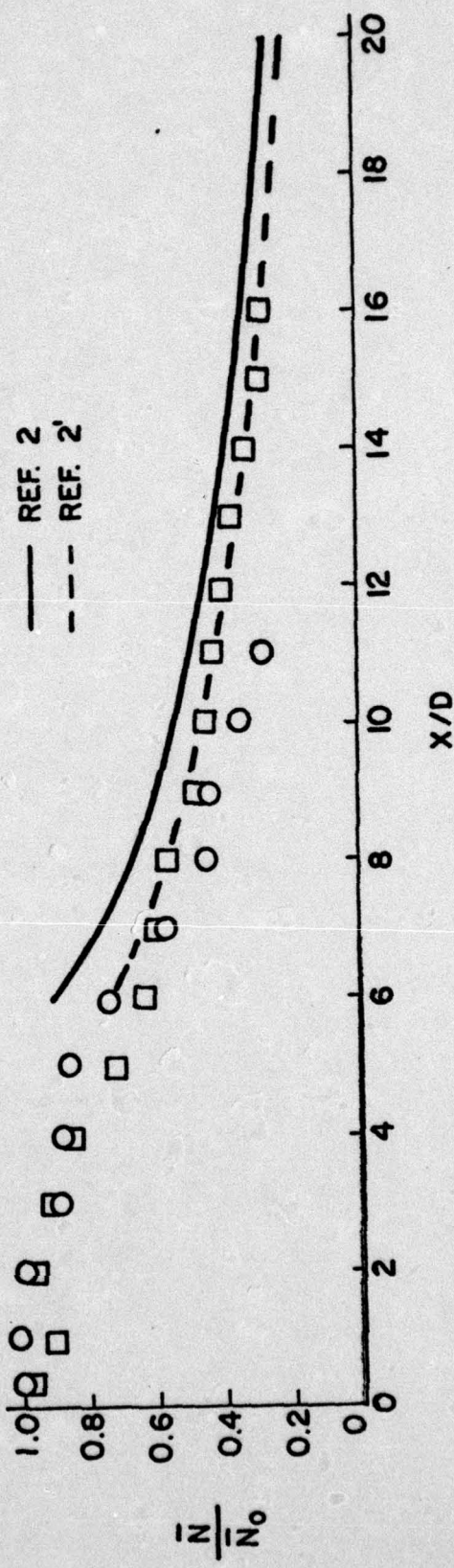


FIG. 4 VELOCITY RATIO VS NORMALIZED AXIAL DISTANCE -  
SINGLE JET

$U_0 = 27.47$  m/sec } PRESENT DATA  
 $U_0 = 12.91$  m/sec }  $CO_2$  SPECIE



**FIG. 5 CONCENTRATION RATIO VS NORMALIZED AXIAL DISTANCE - SINGLE JET**

$\Delta$  REF. 4 (COLD JET)       $\circ$  COLD JET -  $U_0 = 13.52$  m/sec } PRESENT DATA  
 $\blacktriangle$  REF. 4' (FLAME JET)     $\square$  FLAME JET -  $U_0 = 13.71$  m/sec }  
 - - - REF. 9  
 ..... REF. 10  
 — REF. 17

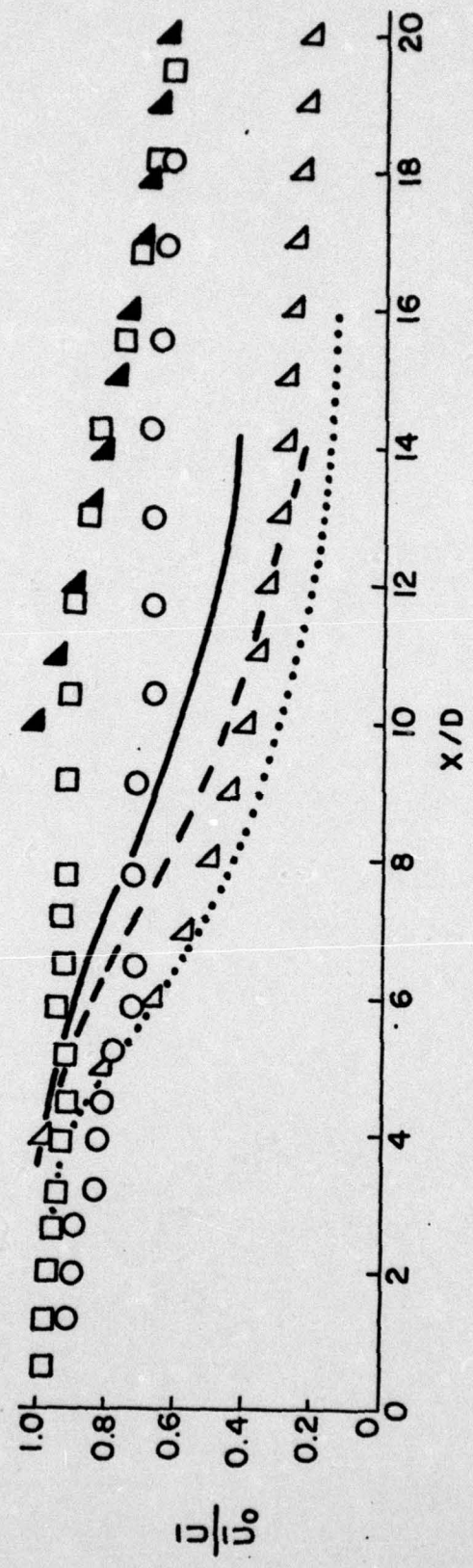


**FIG. 6 VELOCITY RATIO AND TURBULENT INTENSITY VS  
 NORMALIZED AXIAL DISTANCE - COAXIAL JETS**

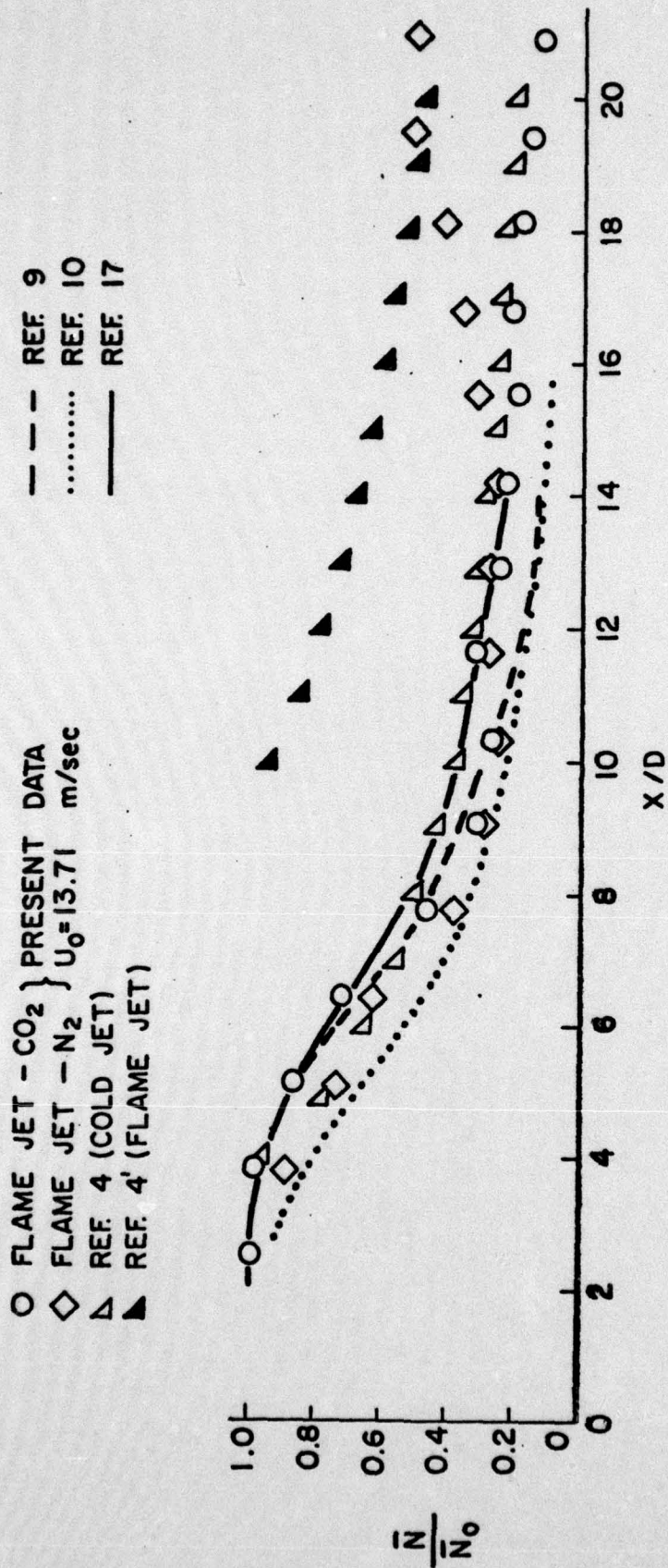
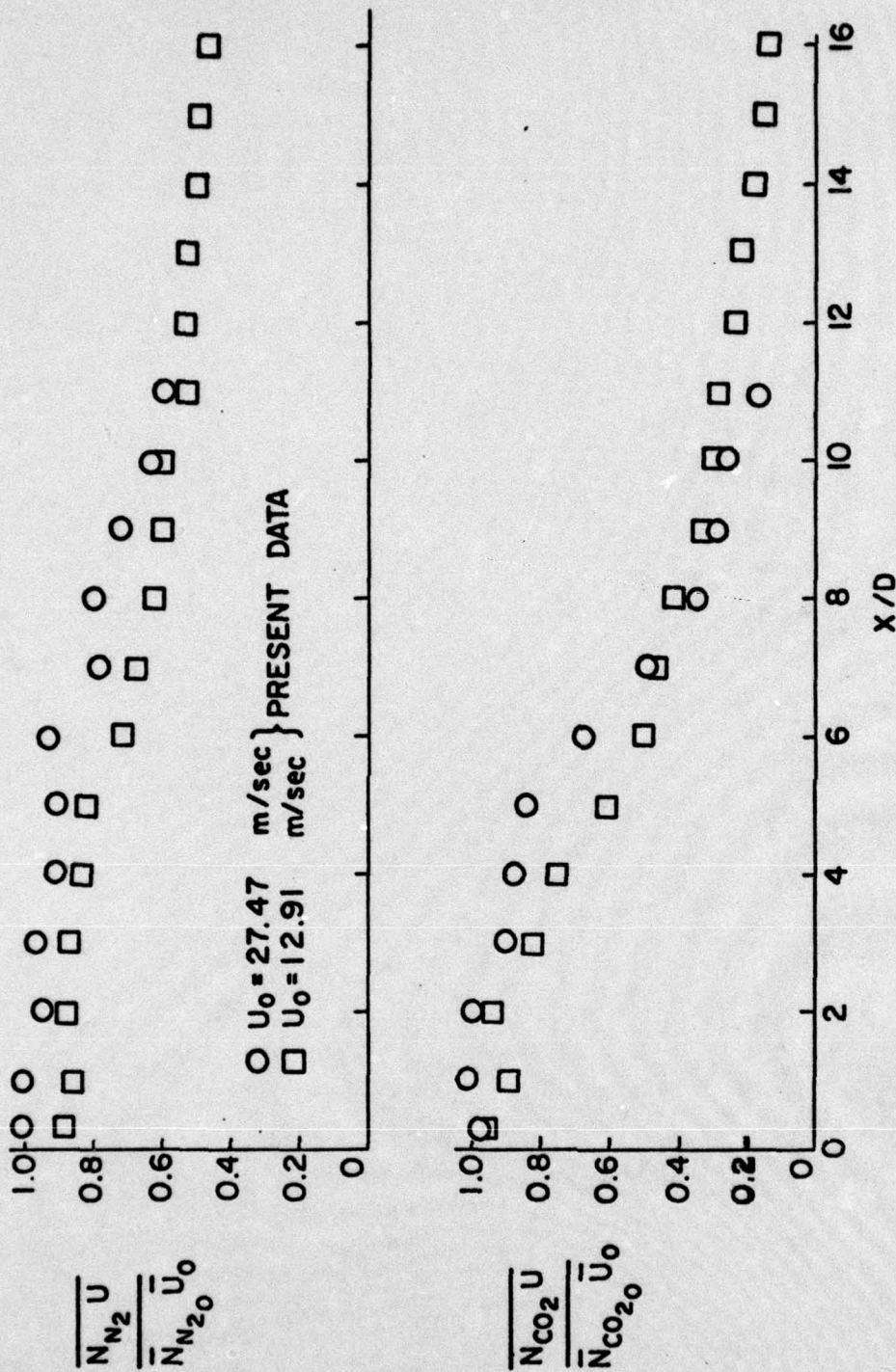


FIG. 7 CONCENTRATION RATIO VS NORMALIZED AXIAL  
 DISTANCE - COAXIAL JET



**FIG. 8 N<sub>2</sub> OR CO<sub>2</sub> CONCENTRATION - VELOCITY MAGNITUDE CORRELATION VS AXIAL DISTANCE - SINGLE JET**

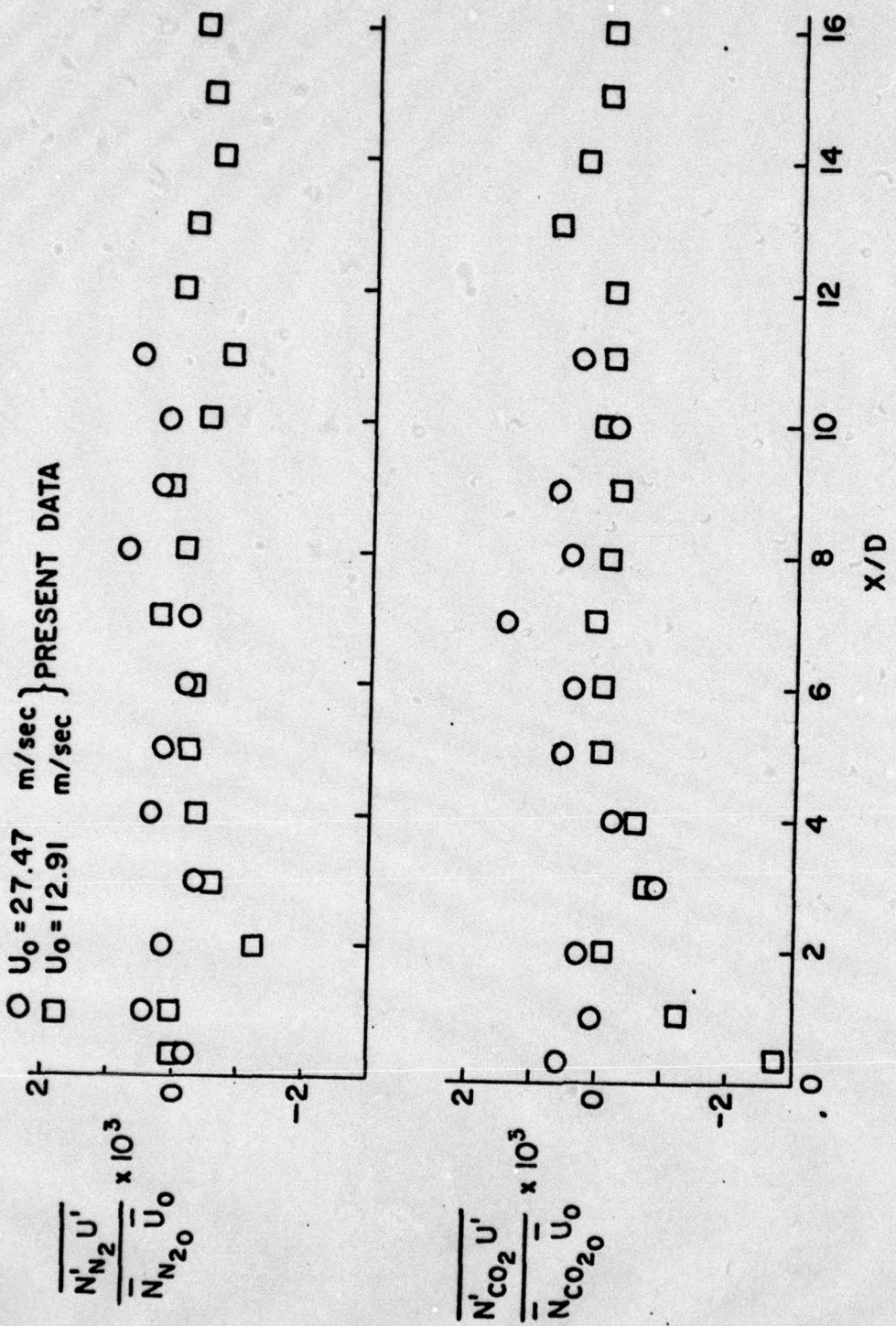
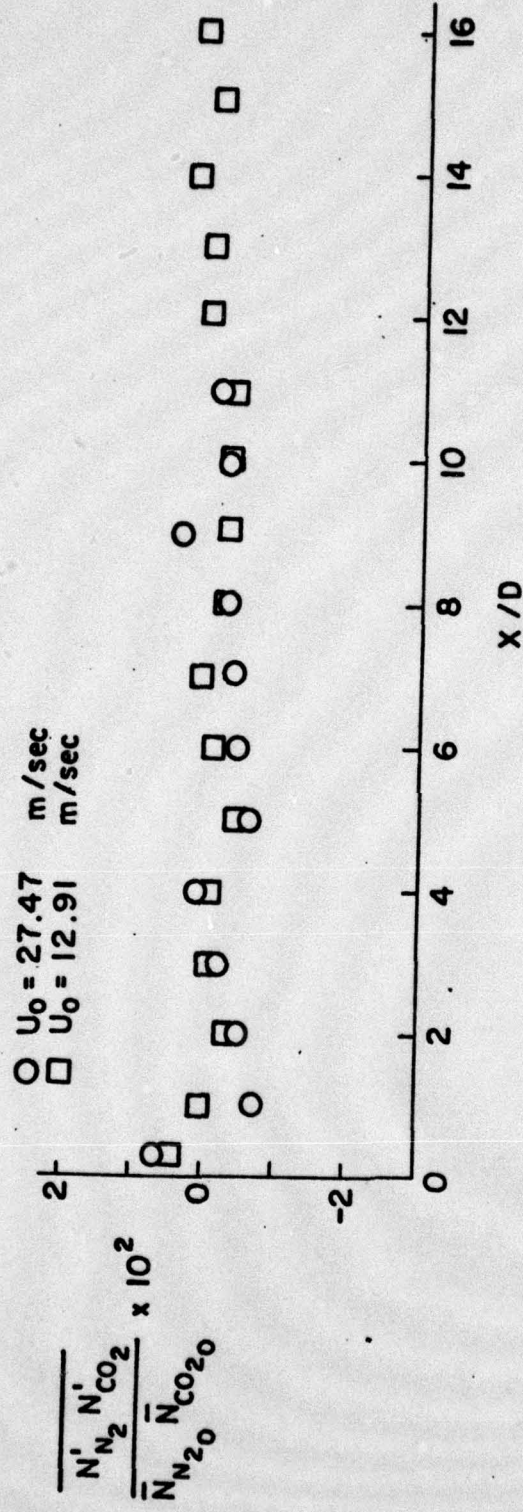
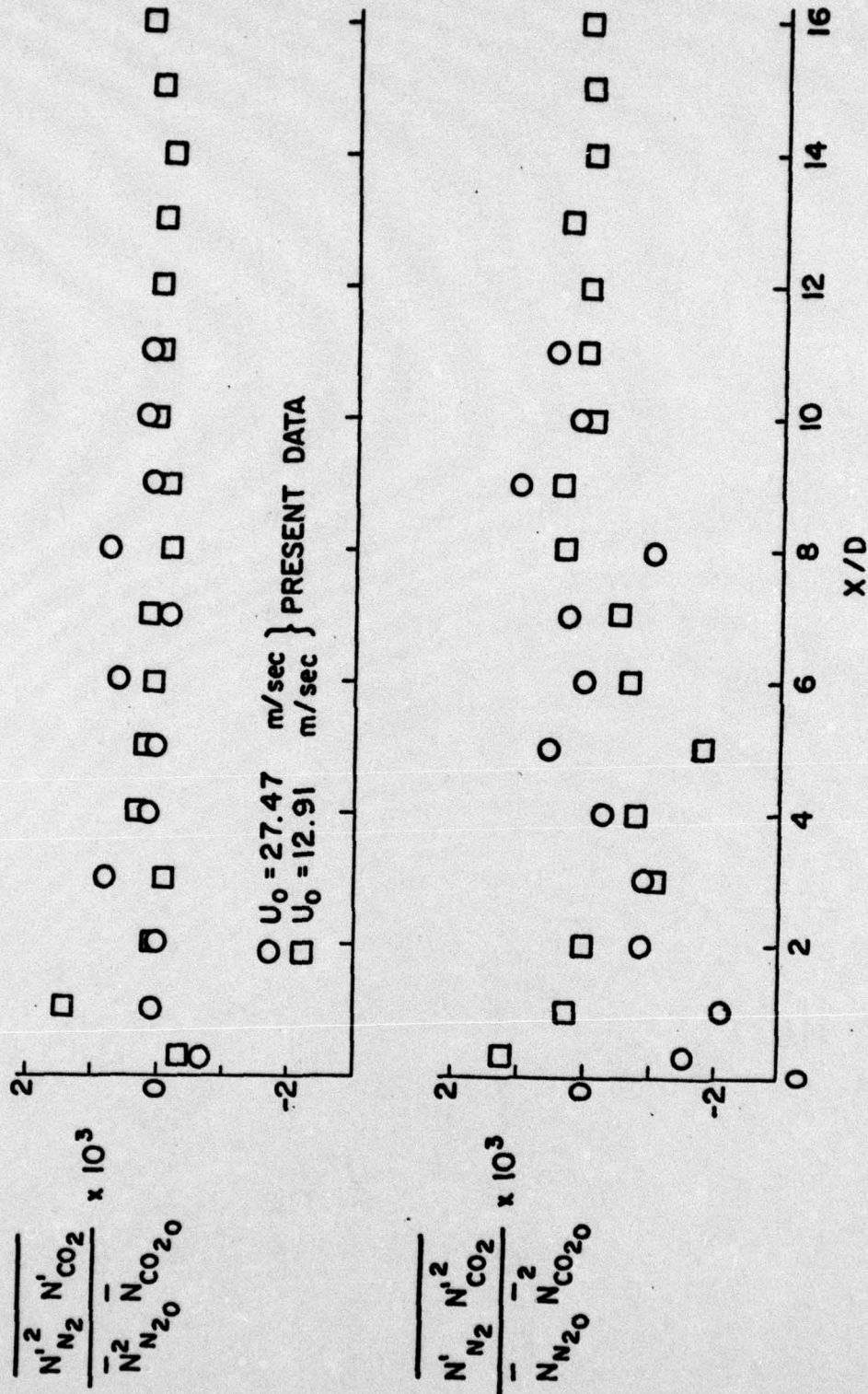


FIG. 9 N<sub>2</sub> OR CO<sub>2</sub> CONCENTRATION - VELOCITY CORRELATION VS NORMALIZED AXIAL DISTANCE - SINGLE JET



**FIG. 10 1<sup>ST</sup> ORDER N<sub>2</sub>-CO<sub>2</sub> CONCENTRATION CORRELATION  
 VS NORMALIZED AXIAL DISTANCE -SINGLE JET**



**FIG. 11 2<sup>ND</sup> ORDER N<sub>2</sub>-CO<sub>2</sub> CONCENTRATION CORRELATION VS NORMALIZED AXIAL DISTANCE - SINGLE JET**

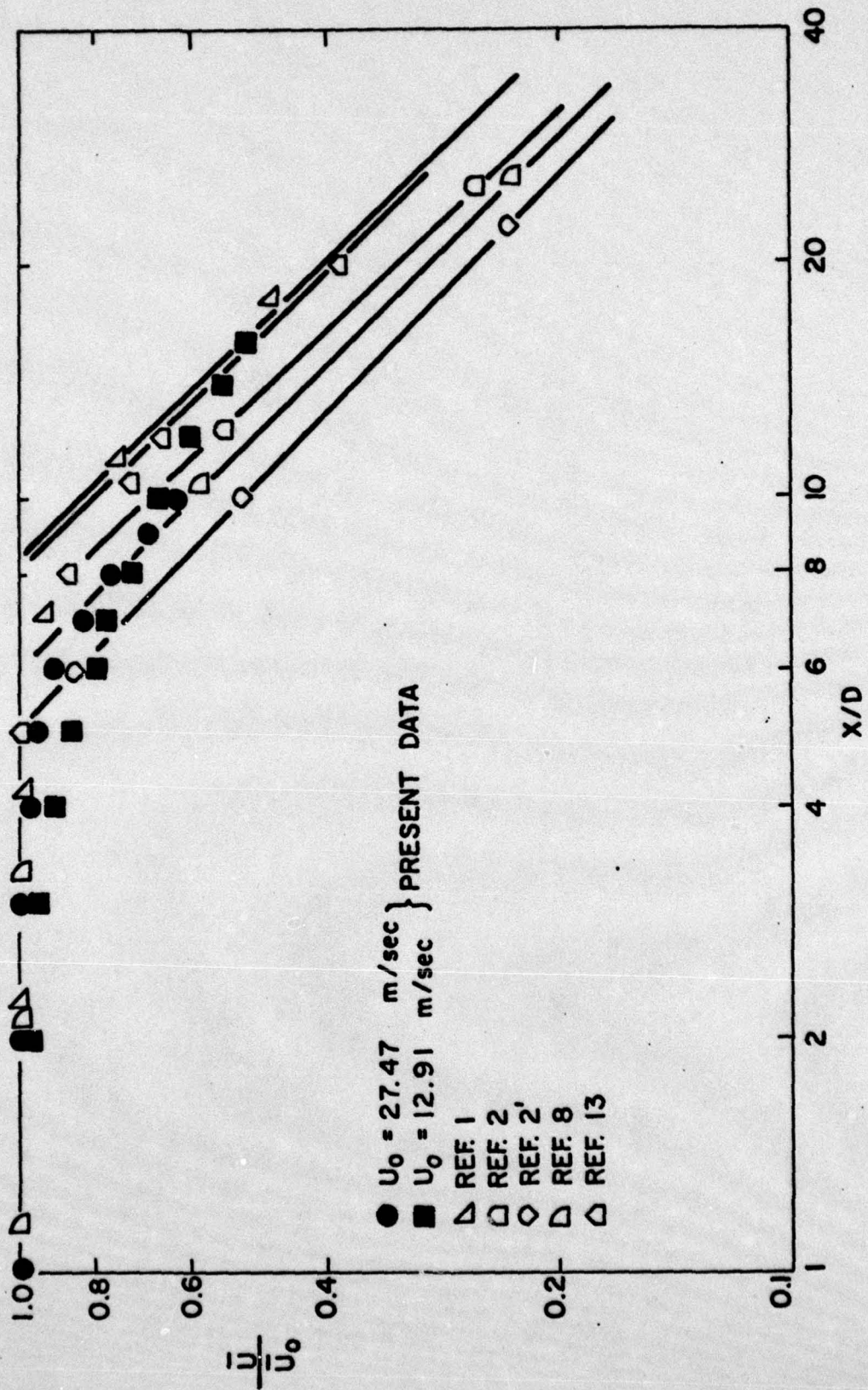


FIG. 12 VELOCITY RATIO VS NORMALIZED AXIAL DISTANCE -  
SINGLE JET

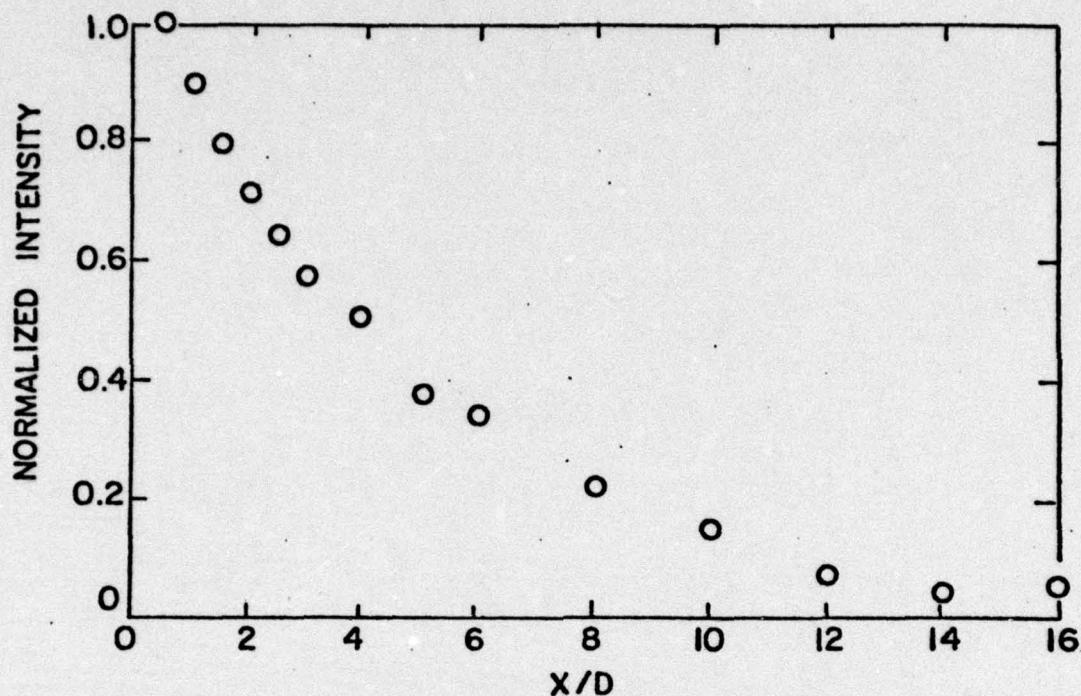


FIG. 13 UNBURNT METHANE NORMALIZED WITH RESPECT TO MAXIMUM

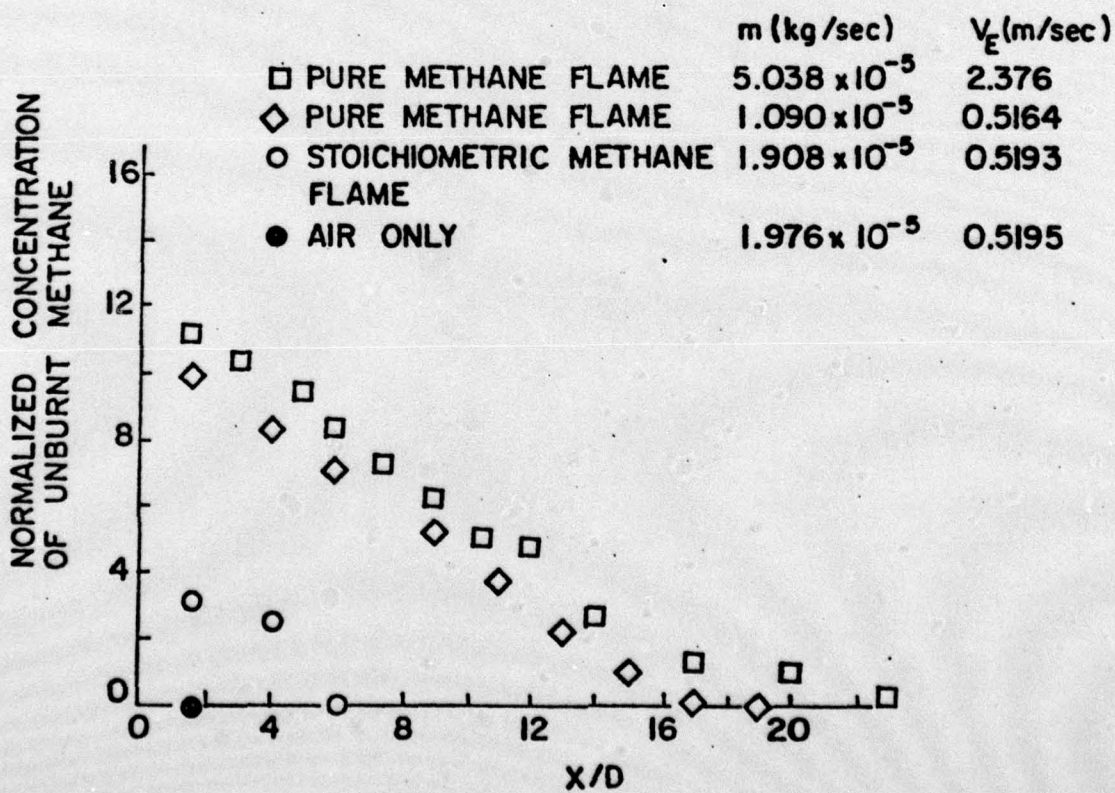


FIG. 14 CONCENTRATION OF UNBURNT METHANE

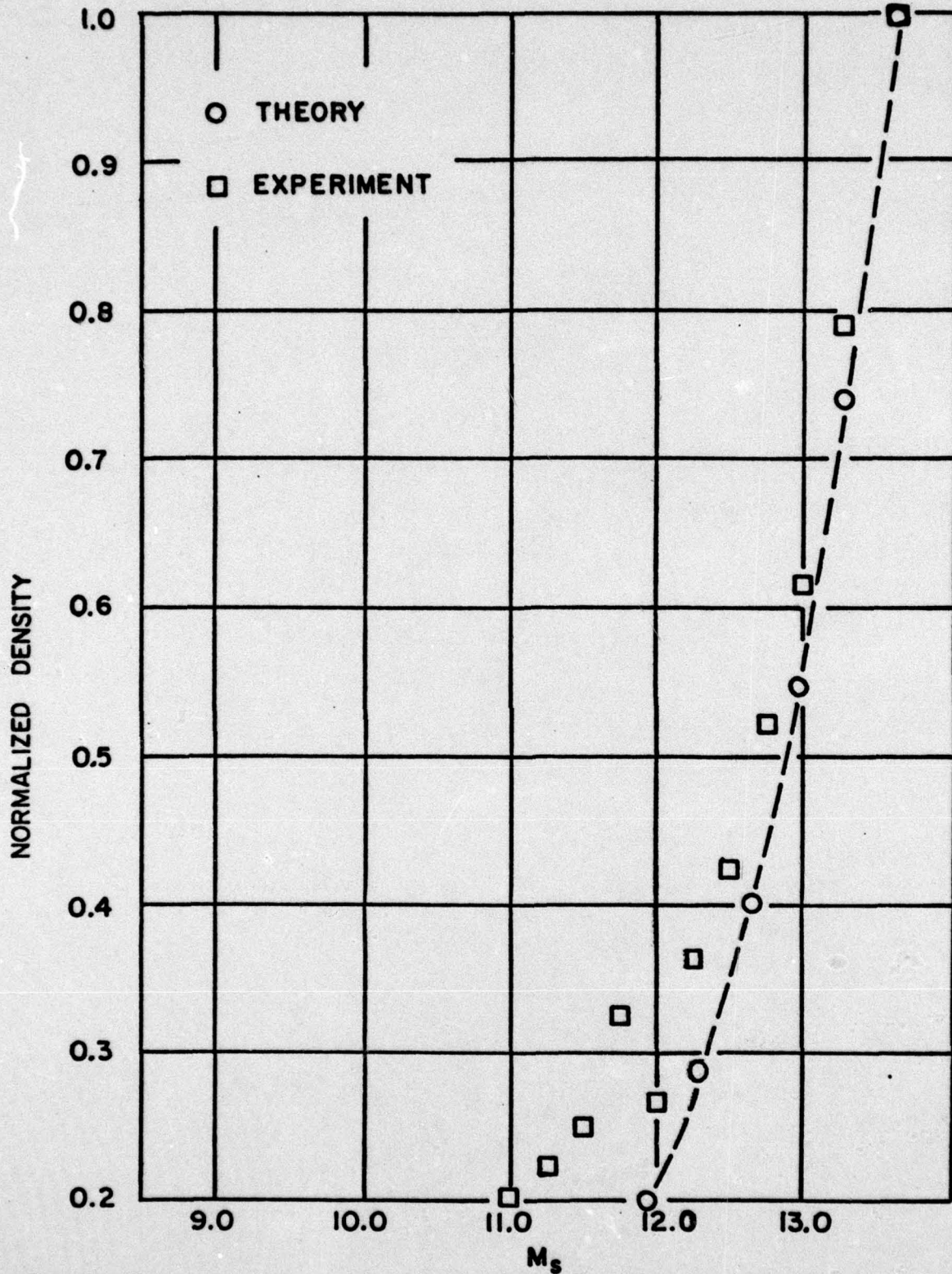


FIG.15 NORMALIZED  $N_2^+$  DENSITY BEHIND REFLECTED SHOCK

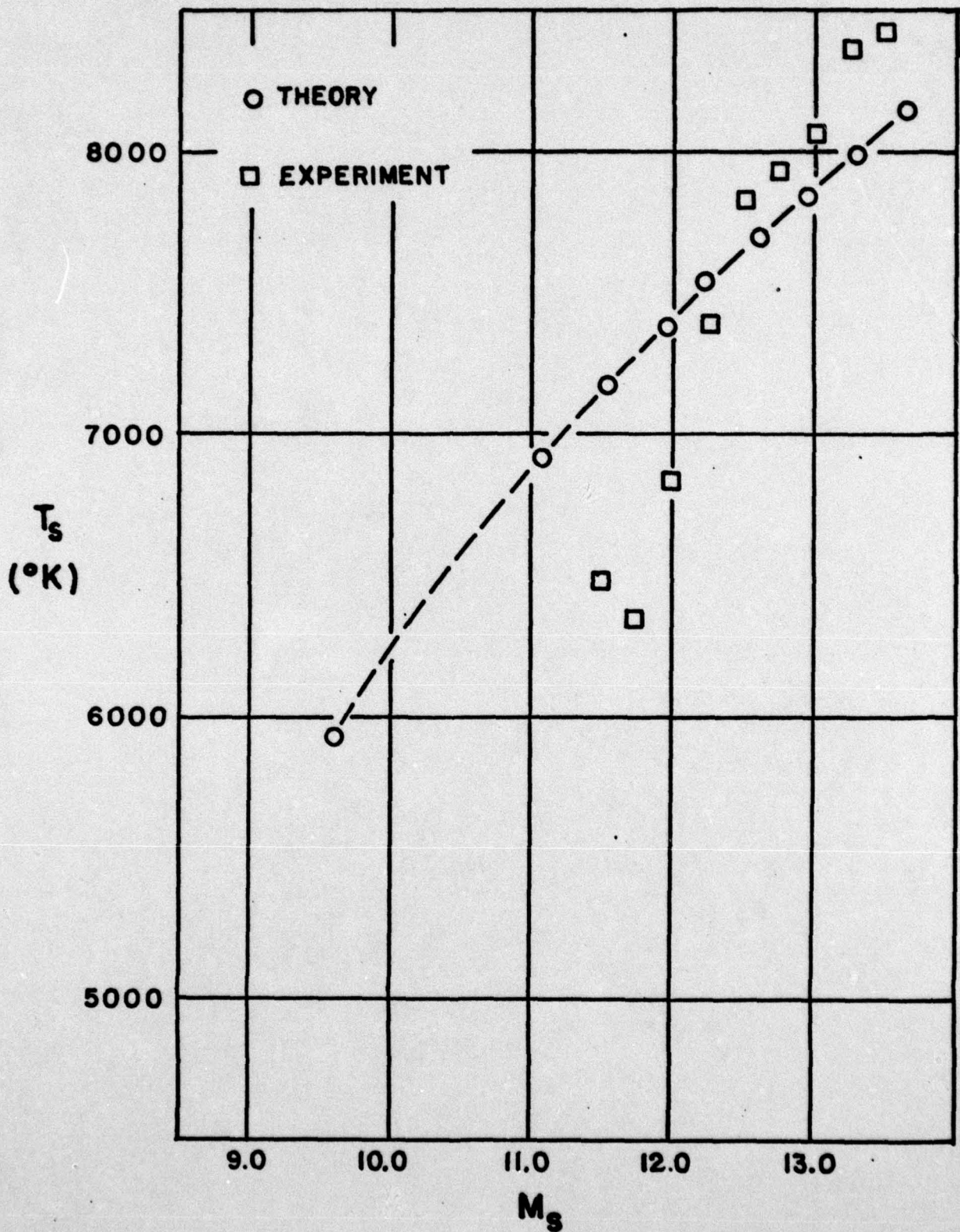


FIG.16 REFLECTED SHOCK TEMPERATURES

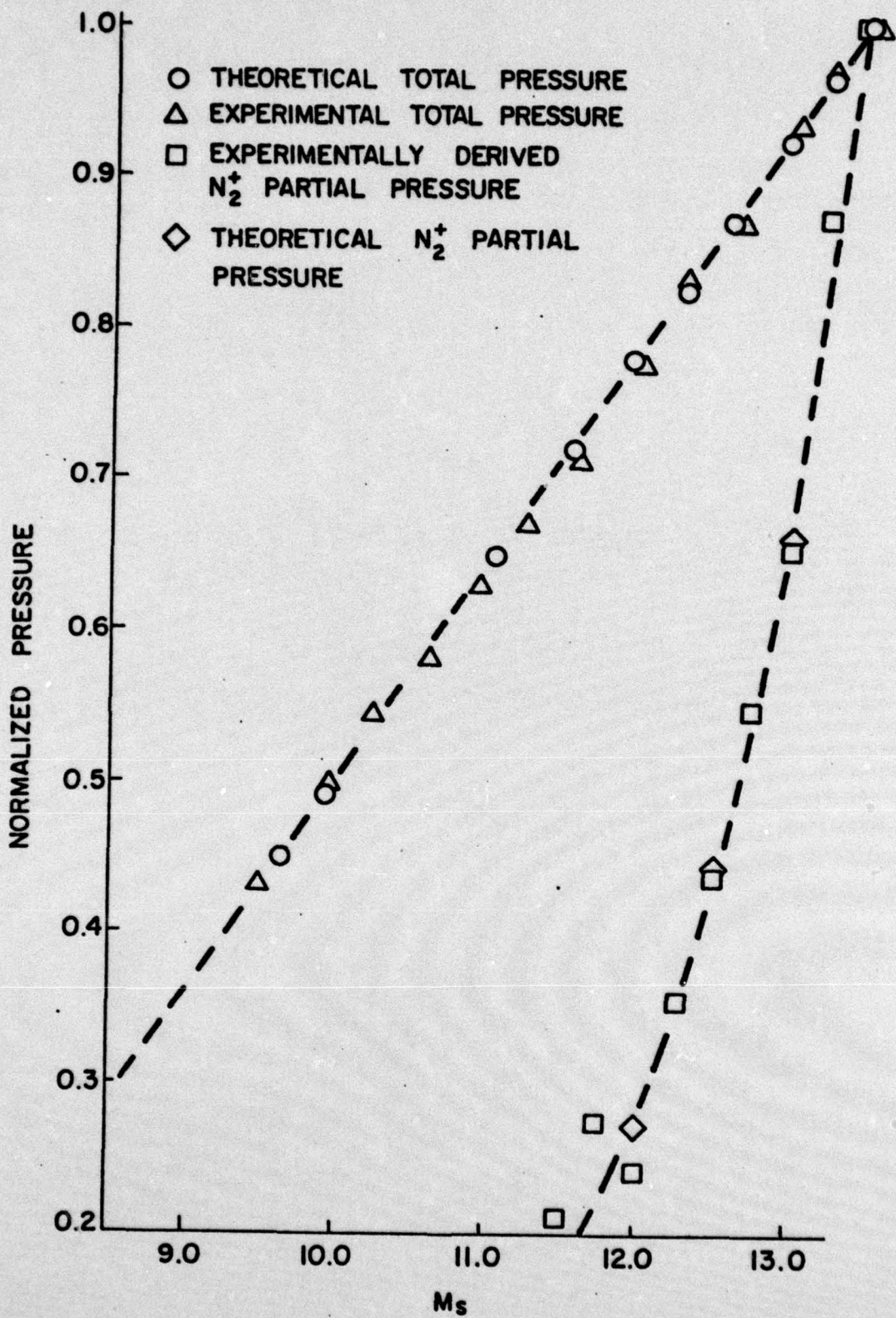


FIG. 17 NORMALIZED PRESSURE

